Hindawi
Journal of Nanomaterials
Volume 2022, Article ID 7181075, 13 pages
https://doi.org/10.1155/2022/7181075

Research Article

Optimization of Plasma Arc Cutting Parameters on Machining of Inconel 718 Superalloy

M. Karthick[1], **P. Anand**[1], **M. Meikandan**[1], **S. Sekar**[2], **L. Natrayan**[3] and **Ketema Bobe**[4]

[1]*Department of Mechanical Engineering, Vel Tech Rangarajan Dr. Sagunthala R&D Institute of Science and Technology, Chennai, Tamilnadu, India*
[2]*Department of Mechanical Engineering, Rajalakshmi Engineering College, Rajalakshmi Nagar, Thandalam, Chennai, 602 105 Tamilnadu, India*
[3]*Department of Mechanical Engineering, Saveetha School of Engineering, SIMATS, Chennai, Tamil Nadu 602105, India*
[4]*Department of Mechanical Engineering, Ambo University, Ambo, Ethiopia*

Correspondence should be addressed to M. Karthick; karthickm@veltech.edu.in, P. Anand; dranand@veltech.edu.in, L. Natrayan; natrayanphd@yahoo.com, and Ketema Bobe; ketema.bobe@ambou.edu.et

Received 17 April 2022; Revised 12 May 2022; Accepted 10 June 2022; Published 20 June 2022

Academic Editor: S.K. Khadheer Pasha

Nickel-based super composites are widely applied in the industry. These alloys withstand high thermal debility conditions and give better strength to machine parts in aviation, biomechanical, marine, and vehicle commerce. Nickel-based alloys have high quality, corrosion resistance, and high heat refusal. Inconel 718 is one such composite extensively utilized in these loading circumstances because of chemical stability, mechanical friction, high thermal corrosion, and high stability. During the cutting procedure, these qualities will bring a lot of processing issues, for example, surface roughness, machining efficiency, and wear of tool. Plasma arc cutting (PAC) is an upsetting metal-cutting process to perform slicing of hard to cut materials even for complex profiles. The present work analyzes the impact of PAC process factors, for instance, *gas pressure* (GP), *arc current* (AC), *cutting speed* (CS), and *stand-off distance* (SOD) on assessing the *kerf width* (KW), *kerf taper* (KT), and *heat-affected zone* (HAZ) of Inconel 718 superalloy. This work deliberates about the cutting parameters required for the machining of Inconel 718 to provide least surface roughness and low instrument wear. *The experiments conducted to validate the ingenuity of the process are in accordance with the optimal parameter settings necessary for machining purposes. The divergence from actuality has been extremely minimal with a relative error of* 4.45% *for kerf width and* 4.36% *for the extent of heat-affected zone postmachining.*

1. Introduction

The demand for nonconventional materials is growing every day, and the reason for this steady rise is the exquisite properties possessed by these materials such as resistance to extreme temperature levels, resistance to weathering and corrosion when exposed to elements of nature, good resistance to persistent application of load, amiable transition between ductile and brittle phases as temperature declines, and excellent strength to weight ratio. Inconel 718 is one such superalloy which possesses such properties. It being extremely resistant to high temperature levels makes it perfect for application in aerospace and ballistics, nuclear power plants, and gas turbine industries owing to its exceptional material characteristics such as possession of excellent strength to weight ratio at elevated temperatures and being extremely resistant to corrosion, thus leading to longer service life. In the majority of the components in aerospace applications and modern innovative jet engines, almost 50% by weight is fabricated by the usage of Inconel 718. Further similar applications comprise being used in nuclear-powered power plants, deep sea diving and marine engineering fields, food

and health products industry, petrochemical plants, and oil rigs. But along with a lot of advantages, Inconel 718 also has many disadvantages.

Adalarasan et al. analytically studied about the machinability of high-velocity turning operation on Inconel 718. It was discovered that when feed and cutting rates are increased, the rate of heat generation increases, resulting in material weakening at the cutting zone, and the direction of chip flow changes along with the depth of cut [1]. Ananthakumar et al. examine the wear life of the tool material when PCBN tooling is used for finish turning on Inconel 718. Thermal cracks, insert fracture, and chipping were discovered at the highest cutting rate of 450 meters/minute, according to the findings. To achieve a long tool life, uncoated, rounded pullouts with an E25 cutting edge should be used at 0.05 millimeter/rev feed rate, 150 meters/minute cutting speed, and 10 bar fluid pressure. Cutting velocity, feed rate, and tool shape all had a significant effect on tool life, according to ANOVA calculations [2]. In Parida's study, in the case of using a cubic boron nitride cutting tool in high-velocity machining of Inconel 718, the differences in tool surface topology were investigated. It has been determined that the crater wear that was observed on the surface was proportional to the total extent along which the cutting is done. From the results, it has been concluded that the microstructure topography of the cubic boron [3]. In Ananthakumar et al. and Behera et al.'s study, the impact of surface roughness and tool wear on high-velocity machining of Inconel 718 was studied analytically. Following a thorough investigation, it was shown that a quality machined surface can be achieved at both decreased and increased speeds. For each consecutive cutting cycle, the surface may deteriorate due to increased tool wear [2, 4].

Zhao et al. conducted a study to identify the optimal machining parameters needed to machine Inconel 718 in a proper manner. With the help of analysis and optimization techniques, such as the Taguchi approach and Grey-relational analysis [5], the parameters were found in such a way that they had to yield the most minimal value of surface roughness and tool material wear [5]. Ahmad et al. studied about the ultrasonically assisted hybrid machining on Inconel alloys to detect the improvements of machinability in aerospace industry. The machining-initiated residual stress indicated that in UAT, increasingly compressive stresses were produced, assisting with diminishing the net tensile stresses, which were otherwise created in (conventional) machining [6]. Gani et al. studied about the application of opposite examination method to assess the external unevenness after machining of Inconel 718 using LA (laser-assisted) milling. Upon consideration of various least cutting thickness influenced by laser, the model taken under consideration has excellent precision with normal error under 0.5%, and the mean contrast of procedure parameters is under 5% [7]. Maity and Bagal in order to drill microholes in Inconel 718 superalloy used magnetic-suspension spindle system. When compared to traditional EDM, they discovered that the high response frequency of the spindle was the reason for MSSS EDM being used to create microholes in Inconel 718 with optimal efficiency and outstanding quality [8].

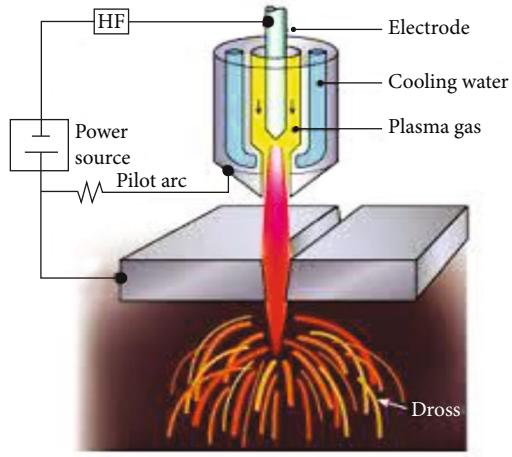

Figure 1: Plasma arc cutting principle.

Devaraj et al. and Fountas et al. proposed a simple method of new tool treatment technique which makes it easy to machine Inconel 718 in turning process. Significant factors derive about chipping and tool failure are elevated levels of friction, temperature levels, and contact force during the machining procedure bring about serious sticking and arrangement of BUE (Built-Up Edge) on the instrument external [9, 10]. Fontanive et al. used micro scale milling assisted with plasma jet at the atmospheric pressure on Inconel 718 to find the process parameters like magnitudes of cutting forces, residual stresses, and surface roughness by using the corresponding techniques. When compared to other cutting methods, the atmospheric compression cold plasma jet using MQL-assisted cutting methods produced the lowest surface roughness value [11]. In Mustafa et al.'s study, in machining Inconel 718 with a noncoated WC tool, parameters and chip characteristics such as cutting speed and tool material wear mechanism were studied. At the point, when the cutting speed is expanded, the helix angle seems to be diminished, and a repeated coiled helical chip is formed [12]. Venkatesan et al. investigated experimentally the evaluation of quality of machined surface of Inconel 718 with cutting edge research. One of the most important variables in enabling improved performance cutting operations with superalloys is the geometry of the cutting-edge tool. Roughness measurements revealed that sharp tools increase surface roughness. Hardness estimations did not show critical variety, since the estimation process is constrained to a least depth of 20 μm [13].

Iosub et al.'s metallographic techniques were used to analyze the development of saw-tooth chips while milling Inconel 718. In terms of research, it has been found out that the increase of temperature at which recrystallization occurs is way higher than the temperature observed [14]. In Maity and Bagal's study, the influence of the solid lubricant–aided MQL (minimum quantity lubrication) cooling conditions on the machining properties of Inconel 718 was experimentally examined using the textured tool [15]. Several research on the topic of machining nonconventional superalloys, such

Table 1: Physical properties of Inconel 718.

Properties	Treated solution	Treated and aged solution
Density	0.297 lb/in^3 (8.193 g/cm^3)	0.298 lb/in^3 (8.23 g/cm^3)
Melting range	2500-2600°F	1371-1431°C
Specific gravity	8.20	8.23

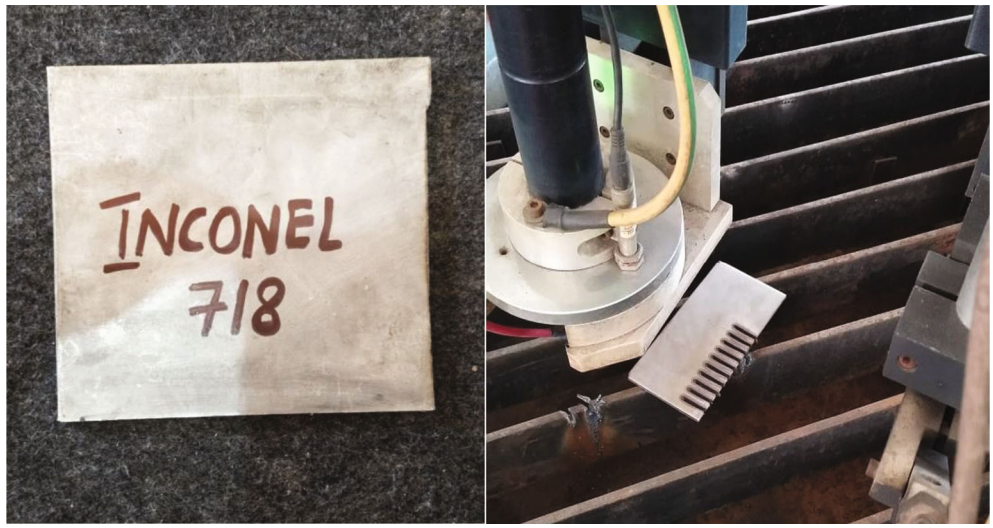

Figure 2: Plasma arc cutting setup and initial stage of the workpiece.

Table 2: The process variables and associated PAC levels.

Parameters	Step 1	Step 2	Step 3
Arc current (Amps)	81	91	101
Cutting speed (meters/minute)	501	751	1001
Gas pressure (Bar)	51	56	61
Stand-off distance (millimeter)	3	4	5

as nickel-based superalloys, have found tool wear processes and changes in surface integrity during the machining process. Many studies have proven that ceramic-based tools are the most optimal ones for machining nickel-based superalloys. [16]. Meikandan and Malarmohan tentatively assessed the kerf quality and HAZ of aluminium composites (sandwich panels) by plasma cutting method. They found out that upon using elevated levels of cutting velocity, the exposure time of plasma on the working surface will be lesser, and the polyethylene core will be less influenced by the heating effects. The kerf quality and HAZ were influenced by the stand of distance. [17]. Bovas Herbert Bejaxhin et al. have suggested a new fuzzy logic approach for evaluating plasma arc cutting qualities and process parameters. When AISI 4140 steel was exposed to plasma arc cutting, they checked the surface roughness. As a result, they were able to recover the dross-free cutting surfaces by raising the cutting speed and workpiece thickness while lowering the arc current. [18]. Karthick et al. investigated the impact of plasma arc cutting on the process parameters on the quality of cut of stainless-steel using hybrid approach in order to assess and estimate the behavior responses under varying machining conditions and parameters. Principal component analysis, grey-relational analysis, and a new type of response surface approach were used [19]. Plasma arc cutting principle is shown in Figure 1.

In Meikandan et al.'s study, on assessing the microhardness, kerf width, and surface roughness of Monel 400 superalloy, they measured experimentally the optimization of plasma arc cutting process parameters like stand-off distance between the plasma torch and work piece surface, pressure of the gas supplied, cutting velocity, and magnitude of arc current [20]. For the machining of innovative and hybrid materials, nontraditional machining technologies have risen in favor in industrial settings. Plasma arc cutting (PAC) is the most common and sought-after nonconventional machining process, with the ability to machine a variety of difficult-to-machine ferrous and nonferrous alloys with impressive cutting velocity, low cost, and the ability to be automated with computational techniques when needed [21–24].

The following table summarizes the physical parameters of Inconel 718.

Many researchers attempted to machine such superalloys by utilizing different conventional machining processes. In these cases, the MRR is extremely low, and it prompts high tooling cost. Since a result, high speediness machining was

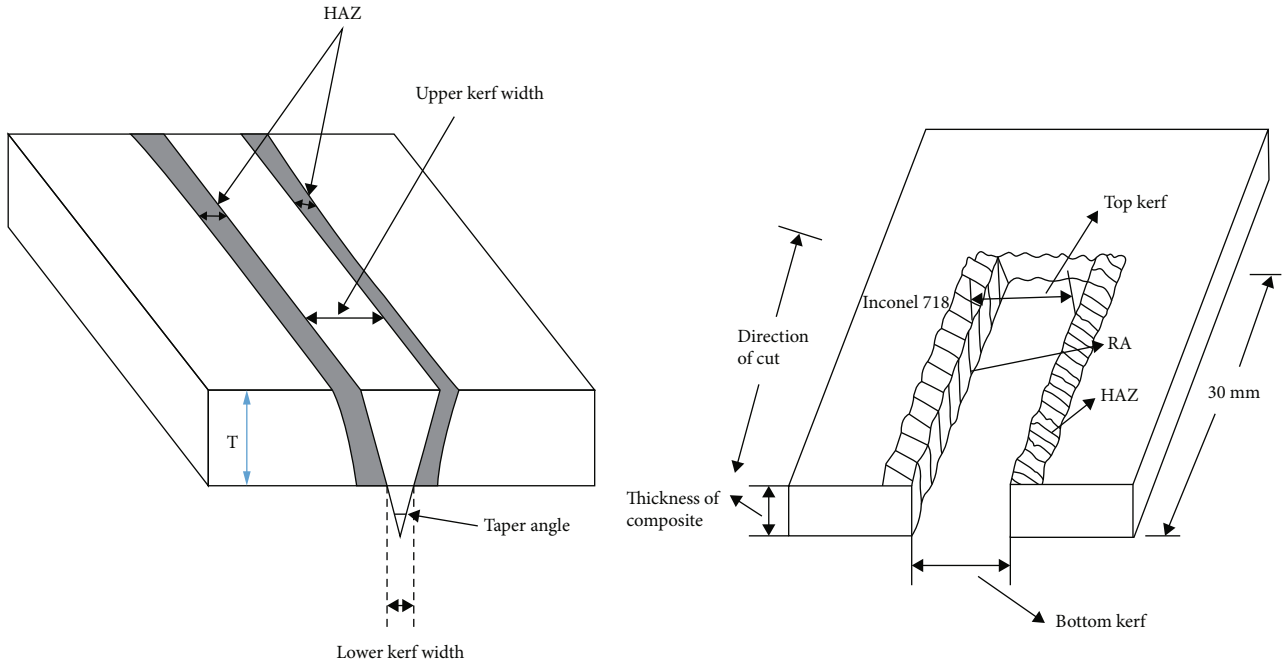

Figure 3: Kerf width, kerf taper, and heat-affected zone.

Figure 4: Plasma arc cutting of Inconel 718.

launched, as demand for quick and efficient machining and superior exterior quality is increasing. High MRR is a significant advantage of high-speed machining, more dissipation of heat, high chip removal rate, and better surface completion. Because of the nature of the task, tool life requirements, and tool material properties, the cutting speed utilised in HSM is frequently 2–50 times faster than that used in traditional (low speed) machining. Being a hybrid material with comparatively less machinability than conventional materials, upon using regular form of machining, the working surface and the subsurface beneath it are damaged and cause serious morphological deformations while machining. To avoid this from happening and to ensure proper surface integrity, the tool selection has to be done in an extremely meticulous manner such as deciding of tool material to use, type and nature of coating that is to be provided, and tool geometry. However, the traditional mechanical cutting process leads to elevated tooling cost while machining of Inconel 718.

1.1. Design of Experiments. Design of experiments (DOE) is the method of design of experiments and iterative processes that help in procuring information that consists of many variations from any particular process. The process is carried out either under the total control of the experimenter or completely oriented to the process itself without enforcing

Table 3: L9–orthogonal array.

Input				Output	
AC (Amps)	CS (meters/minute)	GP (Bar)	SOD (millimeter)	KT (degree)	HAZ (millimeter)
81	501	6	3	7.027	2.71
81	751	56	4	7.923	3.03
81	1001	61	5	8.062	2.93
91	501	56	5	8.821	3.52
91	751	61	3	9.862	3.36
91	1001	51	4	10.984	3.96
101	501	61	4	9.523	3.75
101	751	51	5	9.024	3.64
101	1001	56	3	8.363	4.025

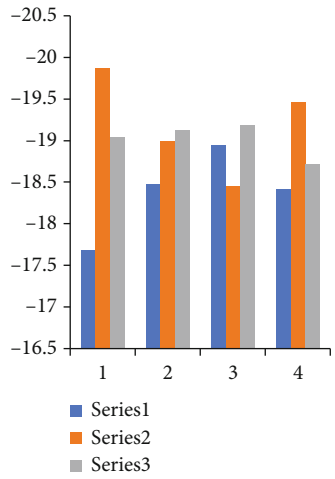

Figure 5: Response table for means for KT.

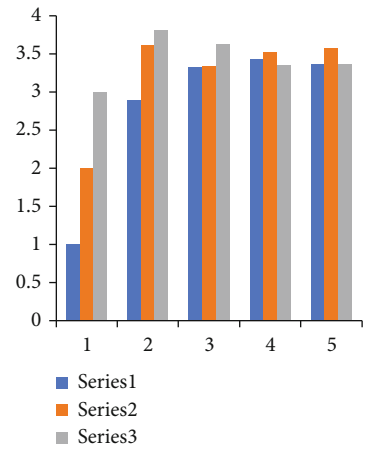

Figure 6: Response table for SD.

control upon the process. The main purpose of the experimenter to implement DOE is to identify variations occurring in any typical process due to interaction of some external factors or due to parametric variations that occur inherently within the process itself [25, 26]. DOE is a well-planned group of experiments in which all controlling factors taken into consideration are varied over a specified range proving as a much better approach to obtain systematic data. Taguchi's orthogonal array experimentation results in a much-controlled variance for the experiment with optimal control parameter settings. An orthogonal array is a sort of experiment in which the columns for the independent variables are orthogonal.

1.2. Taguchi's Orthogonal Array. Quality could be integrated into the manufacturing process by harnessing techniques such as tolerance strategy, system design, and parameter plan. Parameter plan is the methodology by which the primary focus is directed towards determination of optimal process parameters that could be implemented into the manufacturing process. These processes contain long iterative techniques that refine the process parameters to such an extent that the final values procured are the most optimal and could not be further surpassed by any other factors. Quality "inspected into" any specific product refers to production of the required product at all possible quality levels, and if the quality of a peculiar product diverges too much from the desired optimum, then that product is rejected and discarded. Optimal quality is achieved by controlling the divergence of any specific parameter from a desired target. The product design should be formulated is such a manner such that it is resilient against chaotic external factors which we typically have no control over. Thus, the signal-to-noise ratio should be significantly higher [27]. The cost of quality should be assessed as a function of deviation from the planned optimum, and losses should be monitored system wide [28]. This is the idea of the entire loss experienced by the client and society as a result of shortcomings in a low-quality product.

2. Materials and Methods

In the current study, Inconel718 superalloy sheet with a thickness of 5 mm procured from Narendra steels, India,

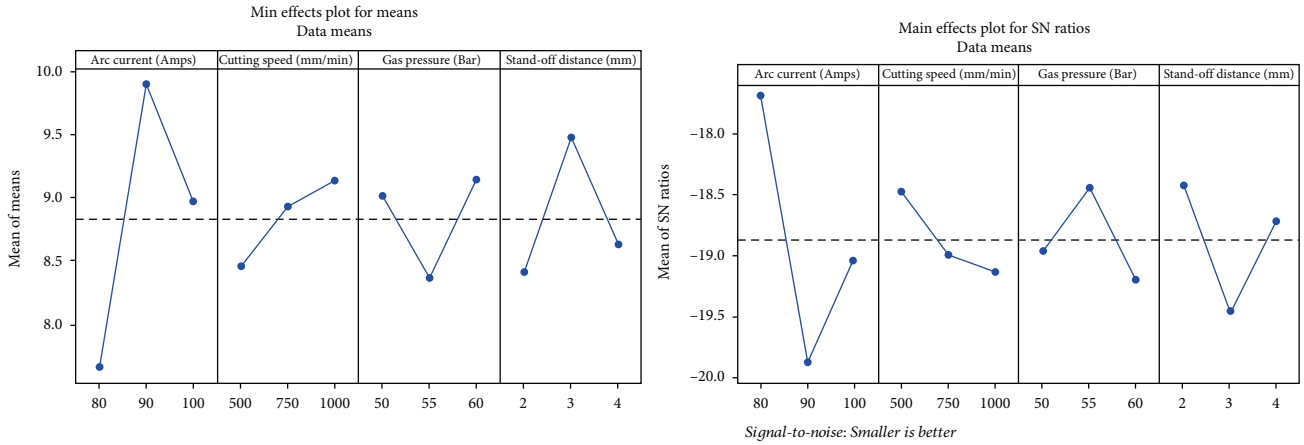

Figure 7: Main effects plot for means and SN ratio data means for KT.

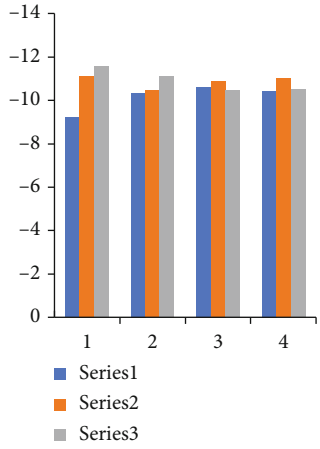

Figure 8: Response table for means for HAZ.

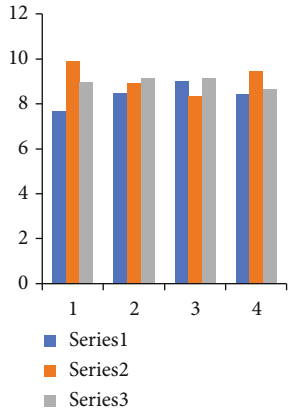

Figure 9: Response table for SD.

has been considered as the workpiece [29]. Table 1 lists the material parameters of the work piece material under consideration. Plasma arc cutting experiments were meticulously carried out using a high-precision CNC plasma cutting machine, as anticipated in advance [30] (Indian manufacturer: Pro arc welding and cutting system Pvt. Ltd.) [31]. The system comes with Plasma CAM CNC software, which allows it to cut work pieces up to 40 millimeters thick at a nozzle traverse speed of 12 meters/minute [32]. A servo-operated torch with a 1.5-millimeter diameter air-cooled swirl nozzle constructed of copper to endure extreme temperatures is used to perform the tedious and extremely precise cutting process [33]. As a shielding gas, atmospheric air is used to create high-energy plasma and blast the melted residue from the work piece surface [34]. Figure 2 shows that plasma arc cutting setup and initial stage of the workpiece.

PAC characteristics including arc current, cutting speed, gas pressure, and stand-off distance are used to measure *kerf width* (KW), *kerf taper* (KT), and *heat-affected zone* (HAZ) [35]. The degree of each variable for the refinement and development of machining quality is determined by a thorough preparatory inquiry, and the relevant parametric data is supplied in Table 2.

Kerf Taper: kerf taper is defined as a half of the kerf width difference per millimeter of depth of cut (or penetration). The formula of the kerf taper is as follows [36]:

$$\text{Kerf taper} = \frac{(\text{TKW} - \text{BKW}) \times 180}{\text{sheet thickness} \times 2\pi}. \quad (1)$$

Heat-Affected Zone: a heat-affected zone is a nonmelted area of metal that has changed material characteristics as a result of being machined at high temperatures.

Optimal quality is achieved by controlling the divergence of any specific parameter from a desired target [37]. The product design should be formulated is such a manner such that it is resilient against chaotic external factors which we typically have no control over. As a result, the signal-to-noise ratio should be much greater [38]. The cost of quality should be quantified as a function of deviation from the targeted optimum, and any losses should be measured system-

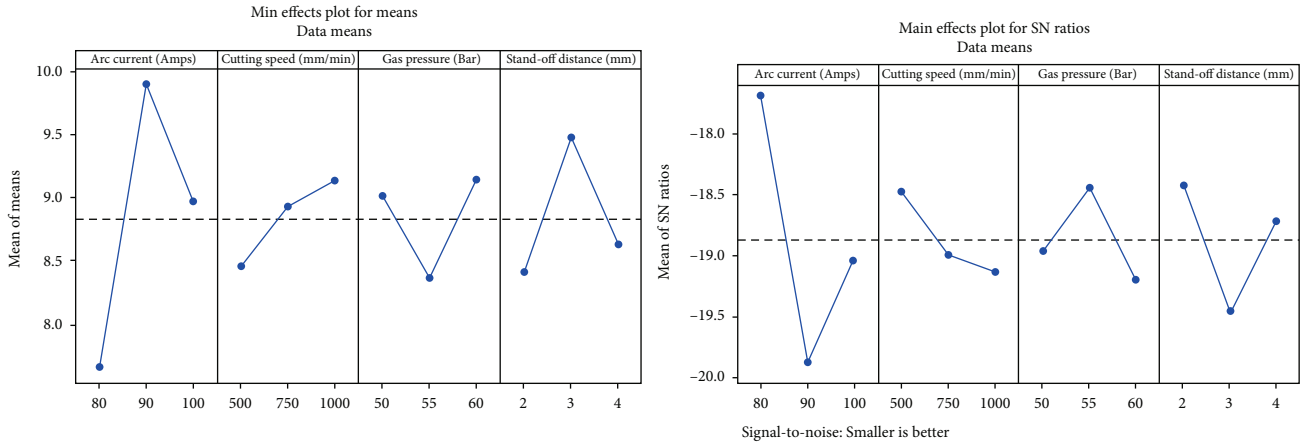

Figure 10: Main effect plot for means and SN ratio data means for HAZ.

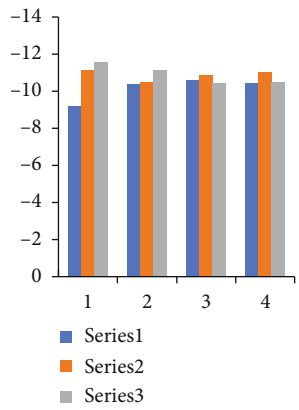

Figure 11: Response table for means.

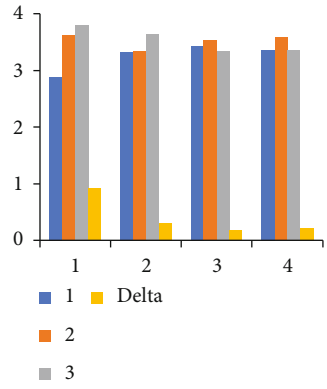

Figure 12: Response table for SD.

wide. This is the idea of the entire loss experienced by the client and society as a result of shortcomings in a low-quality product. Figure 3 shows that kerf width, kerf taper, and heat-affected zone. Plasma arc cutting of Inconel 718 is shown in Figure 4.

3. Result and Discussion

Nine iterative experiments were designed, shown in Table 3, and carried out appropriately in accordance with Taguchi's L9 orthogonal approach to examine the possible convergence and any existing inherent relation between plasma arc cutting process parameters and performance indices such as kerf width postmachining and the extent of the heat-affected zone [39]. The effect of the assumed process components was determined using a second order regression model, and the prediction ability was evaluated using analysis of variance (ANOVA) utilizing Design expert MINITAB software [40]. The results of the ANOVA showed that the quadratic model built using significance and lack of fit tests was suitable. It implies that there is a high degree of convergence between the produced response models and the actual data, demonstrating the models' usefulness.

3.1. Analysis of Empirical Model. Taguchi Analysis: kerf taper (degree) versus arc current … distance (millimeter).

Smaller is preferable in the response table for signal-to-noise ratios.

Figures 5 and 6 show kerf taper (KT) against speed and reflect that kerf taper values are high at low cutting speeds and low at higher cutting speeds.

Figure 7 shows that a lower cutting speed (501 rpm), a faster AC (101 Amps), and a medium GP of 51 bar will result in the least amount of stand of distance.

Taguchi Analysis: HAZ (mm) versus arc current (Amps) and distance (millimeter).

Smaller is preferable in the response table for signal-to-noise ratios.

Figures 8 and 9 show heat-affected zone (HAZ) against speed and reflect that heat-affected zone values are high at low cutting speeds and low at higher cutting speeds.

Figure 10 shows that a higher cutting speed (1001 rpm), a faster AC (101 Amps), and a low GP of 6 bar will result in the least amount of stand of distance. Taguchi Analysis:

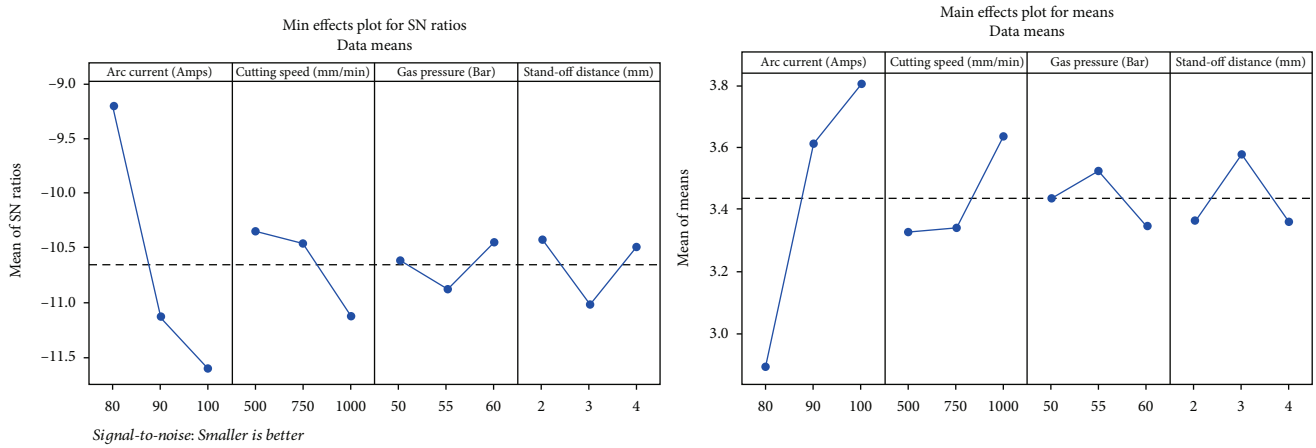

Figure 13: Smaller is preferable in the response table for signal-to-noise ratios.

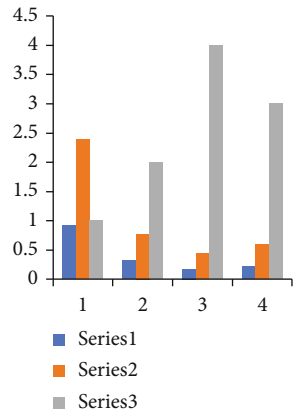

Figure 14: Means from response table.

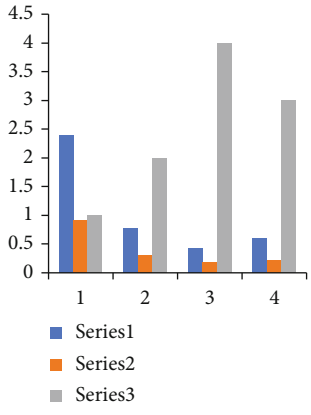

Figure 15: SD from response table.

HAZ (mm) versus arc current (Amps) and distance (millimeter). Smaller is preferable in the response table for signal-to-noise ratios [41].

Figures 11 and 12 show the response table for means and response table for SD for heat-affected zone (HAZ).

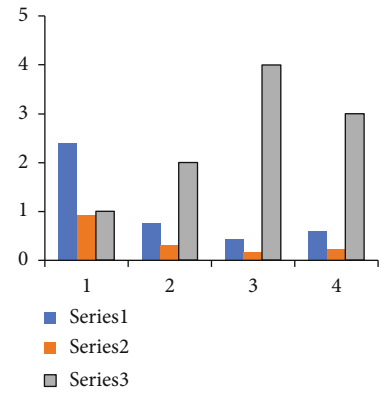

Figure 16: Kerf taper from response table.

Figure 13 shows that smaller is preferable in the response table for signal-to-noise ratios for HAZ.

Taguchi Analysis: kerf taper (degree) and HAZ (mm) versus distance (millimeter). Smaller is preferable in the response table for signal-to-noise ratios. Figures 14, 15, and 16 show the response table for means, SD, and kerf taper.

Figure 17 shows that smaller is preferable in the response table for signal-to-noise ratios for KT and HAZ.

Figure 18 shows the interaction plot for KT data means for arc current, cutting speed, and gas pressure.

Figure 19 shows the interaction plot for HAZ data means for arc current, cutting speed, and gas pressure. Figure 20 shows the contour plot for KT and HAZ.

3.2. Optimization of PAC Parameters. General Linear Model: kerf taper (degree) versus arc … distance (millimeter).

Method

Factor coding(-1, 0, +1)

Factor information

Analysis of variance

Model summary

Coefficients

Table 4 shows the analysis of variance for KT.

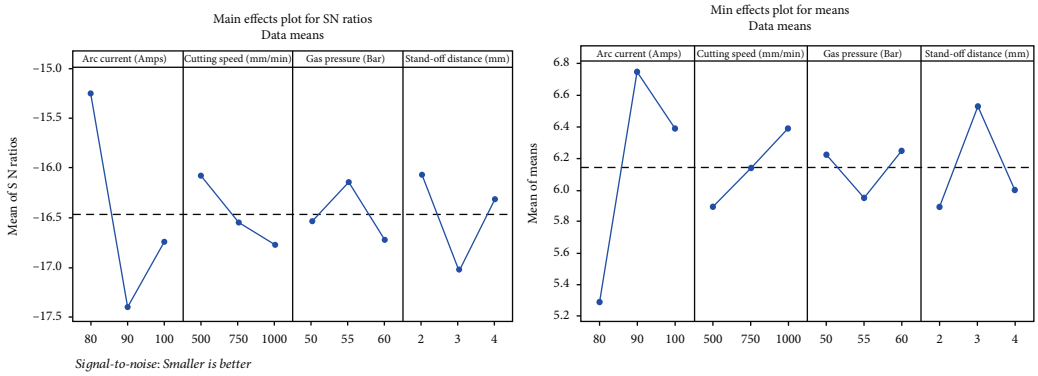

Figure 17: Smaller is preferable in the response table for signal-to-noise ratios.

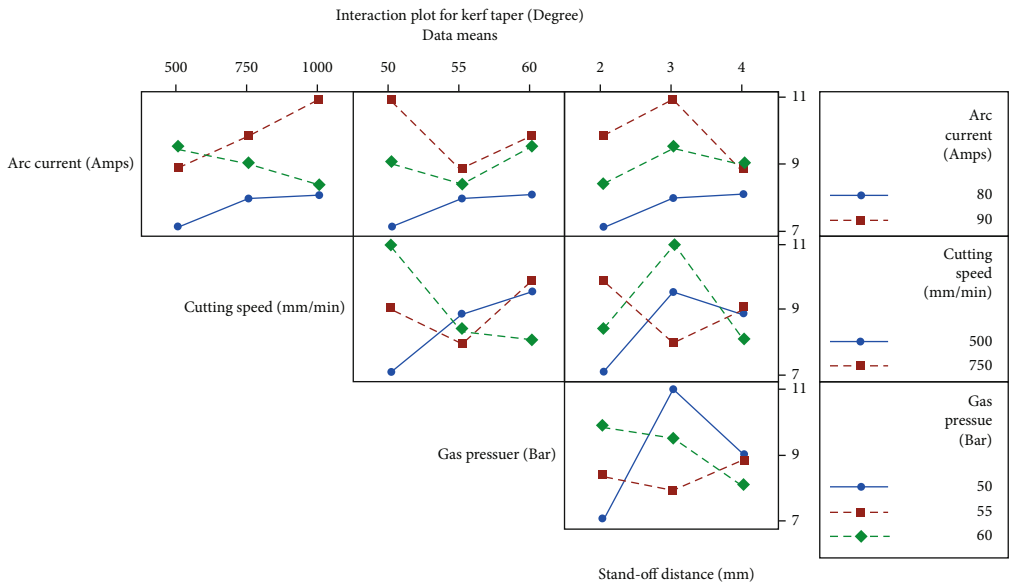

Figure 18: Interaction plot for KT data means.

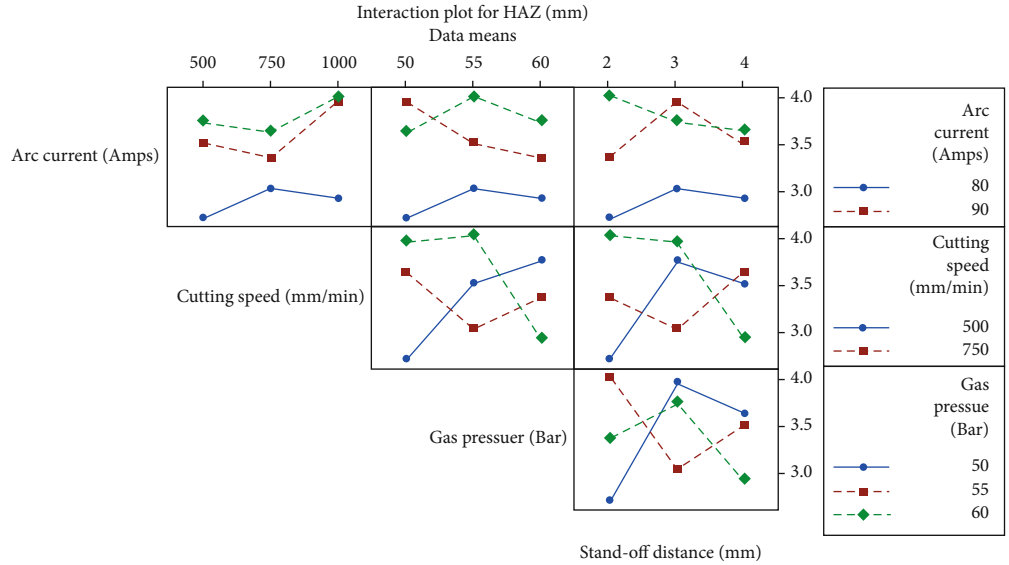

Figure 19: Interaction plot for HAZ data means.

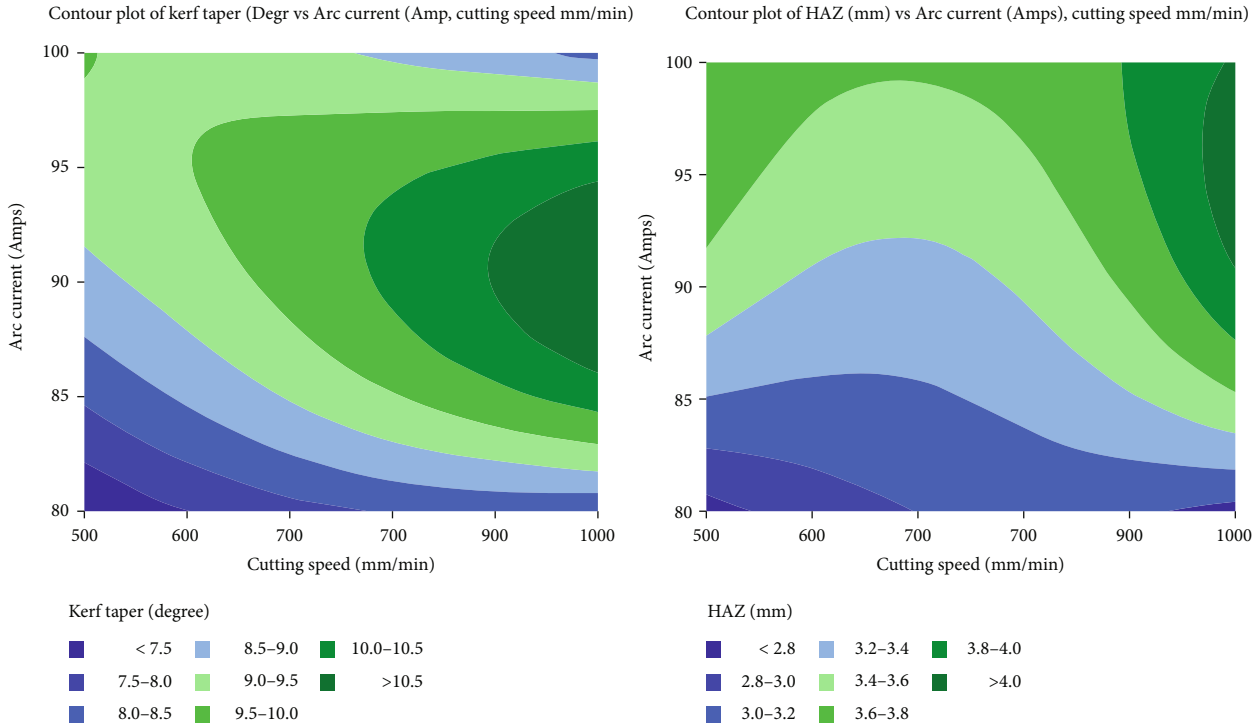

Figure 20: Contour plot for KT and HAZ.

Regression equation

$$\begin{aligned}\mathrm{KT\ (degree)} = {} & 8.843 - 1.173\ \text{arc current (Amps)}_{81} \\ & + 1.046\ \text{arc current (Amps)}_{91} \\ & + 0.1268\ \text{arc current (Amps)}_{101} \\ & - 0.3862\ \text{cutting speed}\left(\frac{\text{millimeter}}{\text{minute}}\right)_{501} \\ & + 0.09311\ \text{cutting speed}\left(\frac{\text{millimeter}}{\text{minute}}\right)_{751} \\ & + 0.2931\ \text{cutting speed}\left(\frac{\text{millimeter}}{\text{minute}}\right)_{1001} \\ & + 0.1684\ \text{gas pressure (Bar))}_{51} \\ & - 0.4742\ \text{gas pressure (Bar)}_{56} \\ & + 0.3058\ \text{gas pressure (Bar)}_{61} - 0.4259\ \text{stand} \\ & - \text{off distance (millimeter))}_{3} + 0.6334\ \text{stand} \\ & - \text{off distance (millimeter)}_{4} - 0.2076\ \text{stand} \\ & - \text{off distance (millimeter)}_{5}.\end{aligned} \tag{2}$$

General Linear Model: HAZ (millimeter) versus arc current … f distance (millimeter).

Method

Regression equation

$$\begin{aligned}\mathrm{HAZ\ (millimeter)} = {} & 3.436 - 0.5461\ \text{arc current (Amps)}_{81} \\ & + 0.1772\ \text{arc current (Amps)}_{91} \\ & + 0.3689\ \text{arc current (Amps)}_{101} \\ & - 0.1094\ \text{cutting speed}\left(\frac{\text{millimeter}}{\text{minute}}\right)_{501} \\ & - 0.09278\ \text{cutting speed}\left(\frac{\text{millimeter}}{\text{minute}}\right)_{751} \\ & + 0.2022\ \text{cutting speed}\left(\frac{\text{millimeter}}{\text{minute}}\right)_{1001} \\ & + 0.000556\ \text{gas pressure (Bar)\_51} \\ & + 0.08889\ \text{gas pressure (Bar)}_{56} \\ & - 0.08944\ \text{gas pressure (Bar)}_{61} \\ & - 0.07111\ \text{stand} - \text{off distance (millimeter)}_{3} \\ & + 0.1439\ \text{stand} - \text{off distance (millimeter)}_{4} \\ & - 0.07278\ \text{stand} - \text{off distance (millimeter)}_{5}.\end{aligned} \tag{3}$$

Regression Analysis: kerf taper (degree) versus arc … ff distance (millimeter).

Analysis of variance

Table 4: Analysis of variance for KT.

Term	Coef	SE Coef	*T*-value	*P* value	VIF
Constant	8.843	*	*	*	
Arc current (Amps)					
80	-1.173	*	*	*	1.33
90	1.046	*	*	*	1.33
Cutting speed (mm/min)					
500	-0.3862	*	*	*	1.33
750	0.09311	*	*	*	1.33
Gas pressure (Bar)					
50	0.1684	*	*	*	1.33
55	-0.4742	*	*	*	1.33
Stand-off distance (mm)					
2	-0.4259	*	*	*	1.33
3	0.6334	*	*	*	1.33

Table 5: Analysis of variance for HAZ.

Source	DF	Adj SS	Adj MS	*F*-value	*P* value
Regression	4.1	1.31370	0.35342	4.58	0.085
Arc current (Amps)	1	1.25584	1.25584	16.27	0.016
Cutting speed (millimeter/minute)	1	0.14570	0.14570	1.89	0.241
Gas pressure (Bar)	1	0.01215	0.01215	0.16	0.712
Stand-off distance (millimeter)	1	0.00000	0.00000	0.00	0.994
Error	4.1	0.30879	0.07720		
Total	8.1	1.72249			

Regression equation

$$\begin{aligned}\text{Kerf taper (degree)} = {} & 0.89 + 0.0650\,\text{arc current (Amps)} \\ & + 0.00136\,\text{cutting speed}\left(\frac{\text{mm}}{\text{min}}\right) \\ & + 0.014\,\text{gas pressure (Bar)} \\ & + 0.109\,\text{stand} - \text{off distance (millimeter)}.\end{aligned} \tag{4}$$

Regression Analysis: HAZ (millimeter) versus arc current ff distance (millimeter).

Analysis of variance.

Table 5 shows the analysis of variance for HAZ.

Model summary.

Coefficients.

Regression equation

$$\begin{aligned}\text{HAZ (millimeter)} = {} & -0.65 + 0.0458\,\text{arc current (Amps)} \\ & + 0.000623\,\text{cutting speed}\left(\frac{\text{millimeter}}{\text{minute}}\right) \\ & - 0.0090\,\text{gas pressure (Bar)} \\ & - 0.001\,\text{stand} - \text{off distance (millimeter)}.\end{aligned} \tag{5}$$

4. Conclusion

In the current study, the effect of significant plasma arc cutting input and output parameters on postmachining properties of Inconel 718 superalloy such as kerf width, heat-affected zone, and kerf taper has been scrutinized thoroughly by the help of appropriate experimentation techniques and optimization attempts. The key observations are as follows:

(i) After conducting analysis of variance on the values of the procured parameters, it has been found out that kerf width and stand-off distance are influenced by velocity of cutting and supply pressure of gas

(ii) The regression analysis models between the heat affected zone postmachining and kerf width have achieved a confidence level of 95% which has been deemed adequate to finalize a relation between the selected parameters

(iii) The experiments conducted to validate the ingenuity of the process are in accordance with the optimal parameter settings necessary for machining purposes

(iv) The divergence from actuality has been extremely minimal with a relative error of 4.45% for kerf width and 4.36% for the extent of heat-affected zone postmachining

(v) Thus, the selected method is deemed optimal as it meets all the requirements necessary for an optimal process

(vi) On conducting a morphological study to gauge the material and surface characteristics of the superalloy, it has been found out that an increase in pressure of the supplied gas results in the formation of dross attachments and striation patterns on the alloy

(vii) This results in a decline of the cut quality and could be countered by the help of a reduced magnitude of arc current and an increased gas pressure

Future scopes of the work are as follows:

(i) The experimental works on machinability assessment of Inconel 718 can be extended to other heat resistant superalloys

(ii) Further machinability assessment of Inconel 718 and other responses like power consumption, temperature, machining sound, and tool vibration can also be considered along with responses, used in this research

(iii) Other parameters such as tool nose radius, cutting angle, and rake angle can also be considered in modelling and optimization

(iv) On-line tool wear monitoring system can also be incorporated in the future research

(v) Performance of carbide tool in contour turning can be considered for the further research

Data Availability

The data used to support the findings of this study are included within the article. Should further data or information be required, these are available from the corresponding author upon request.

Conflicts of Interest

The authors declare that there are no conflicts of interest regarding the publication of this paper.

Acknowledgments

The authors thank Vel Tech Rangarajan Dr. Sagunthala R&D Institute of Science and Technology, Chennai and Saveetha School of Engineering, SIMATS, Chennai, Tamilnadu, for the technical assistance. The authors appreciate the support from the Ambo University, Ethiopia.

References

[1] R. Adalarasan, M. Santhanakumar, and M. Rajmohan, "Application of Grey Taguchi –based response surface methodology (GT-RSM) for optimizing the plasma arc cutting parameters of 304L stainless steel," *The International Journal of Advanced Manufacturing Technology*, vol. 78, no. 5, pp. 1161–1170, 2015.

[2] K. Ananthakumar, D. Rajamani, E. Balasubramanian, and J. Paulo Davim, "Measurement and optimization of multi-response characteristics in plasma arc cutting of Monel 400™ using RSM and TOPSIS," *Measurement*, vol. 135, pp. 725–737, 2019.

[3] A. K. Parida, "Analysis of chip geometry in hot machining of Inconel 718 alloy," *Iranian Journal of Science and Technology, Transactions of Mechanical Engineering*, vol. 43, no. S1, pp. 155–164, 2019.

[4] B. C. Behera, S. G. Chetan, and V. R. Paruchuri, "Study of saw-tooth chip in machining of Inconel 718 by metallographic technique," *Machining Science and Technology*, vol. 23, no. 3, pp. 431–454, 2019.

[5] B. Zhao, H. Liu, C. Huang, J. Wang, B. Wang, and Y. Hou, "Cutting performance and crack self-healing mechanism of a novel ceramic cutting tool in dry and high-speed machining of Inconel 718," *The International Journal of Advanced Manufacturing Technology*, vol. 102, no. 9-12, pp. 3431–3438, 2019.

[6] S. Ahmad, R. M. Singari, and R. S. Mishra, "Tri-objective constrained optimization of pulsating DC sourced magnetic abrasive finishing process parameters using artificial neural network and genetic algorithm," *Materials and Manufacturing Processes*, vol. 36, no. 7, pp. 843–857, 2021.

[7] A. Gani, W. Ion, and E. Yang, "Experimental investigation of plasma cutting two separate thin steel sheets simultaneously and parameters optimisation using Taguchi approach," *Journal of Manufacturing Processes*, vol. 64, pp. 1013–1023, 2021.

[8] N. Pragadish, S. Kaliappan, M. Subramanian et al., "Optimization of cardanol oil dielectric-activated EDM process parameters in machining of silicon steel," *Biomass Conversion and Biorefinery*, vol. 12, pp. 1–10, 2022.

[9] R. Devaraj, E. Abouel Nasr, B. Esakki, A. Kasi, and H. Mohamed, "Prediction and analysis of multi-response characteristics on plasma arc cutting of Monel 400™ alloy using Mamdani-fuzzy logic system and sensitivity analysis," *Materials*, vol. 13, no. 16, p. 3558, 2020.

[10] N. A. Fountas, J. D. Kechagias, A. C. Tsiolikas, and N. M. Vaxevanidis, "Multi-objective optimization of printing time and shape accuracy for FDM-fabricated ABS parts," *Metaheuristic. Computing. And. Applications.*, vol. 1, no. 2, pp. 115–129, 2020.

[11] F. Fontanive, R. P. Zeilmann, and J. D. Schenkel, "Surface quality evaluation after milling Inconel 718 with cutting edge preparation," *The International Journal of Advanced Manufacturing Technology*, vol. 104, no. 1-4, pp. 1087–1098, 2019.

[12] G. Mustafa, J. Liu, F. Zhang et al., "Atmospheric pressure plasma jet assisted micro-milling of Inconel 718," *The International Journal of Advanced Manufacturing Technology*, vol. 103, no. 9-12, pp. 4681–4687, 2019.

[13] K. Venkatesan, R. Ramanujam, and P. Kuppan, "Investigation of machinability characteristics and chip morphology study in laser-assisted machining of Inconel 718," *The International Journal of Advanced Manufacturing Technology*, vol. 91, no. 9-12, pp. 3807–3821, 2017.

[14] A. Iosub, G. Nagit, and F. Negoescu, "Plasma cutting of composite materials," *International Journal of Material Forming*, vol. 1, no. S1, pp. 1347–1350, 2008.

[15] K. P. Maity and D. K. Bagal, "Effect of process parameters on cut quality of stainless steel of plasma arc cutting using hybrid approach," *The International Journal of Advanced Manufacturing Technology*, vol. 78, no. 1-4, pp. 161–175, 2015.

[16] M. Meikandan, M. Karthick, L. Natrayan et al., "Experimental investigation on tribological behaviour of various processes of anodized coated piston for engine application," *Journal of Nanomaterials*, vol. 2022, Article ID 7983390, 8 pages, 2022.

[17] M. Meikandan and K. Malarmohan, "Fabrication of a superhydrophobic nanofibres by electrospinning," *Digest Journal of Nanomaterials and Biostructures*, vol. 12, no. 1, pp. 11–17, 2021.

[18] A. Bovas Herbert Bejaxhin, G. Paulraj, G. Jayaprakash, and V. Vijayan, "Measurement of roughness on hardened D-3 steel and wear of coated tool inserts," *Transactions of the Institute of Measurement and Control*, vol. 43, no. 3, pp. 528–536, 2021.

[19] M. Karthick, P. Anand, M. Meikandan, and M. Siva Kumar, "Machining performance of Inconel 718 using WOA in PAC," *Materials and Manufacturing Processes*, vol. 36, no. 11, pp. 1274–1284, 2021.

[20] M. Meikandan, M. Sundarraj, D. Yogaraj, and K. Malarmohan, "Experimental and numerical investigation on bare tube cross flow heat exchanger-using COMSOL," *International Journal of Ambient Energy*, vol. 41, no. 5, pp. 500–510.

[21] M. Rakesh and S. Datta, "Effects of cutting speed on chip characteristics and tool wear mechanisms during dry machining of Inconel 718 using uncoated WC tool," *Arabian Journal for Science and Engineering*, vol. 44, no. 9, pp. 7423–7440, 2019.

[22] Y. Sesharao, T. Sathish, K. Palani et al., "Optimization on operation parameters in reinforced metal matrix of AA6066 composite with HSS and Cu," *Advances in Materials Science and Engineering*, vol. 2021, Article ID 1609769, 12 pages, 2021.

[23] D. Damodharan, K. Gopal, A. P. Sathiyagnanam, B. Rajesh Kumar, M. V. Depoures, and N. Mukilarasan, "Performance and emission study of a single cylinder diesel engine fuelled withn-octanol/WPO with some modifications," *International Journal of Ambient Energy*, vol. 42, no. 7, pp. 779–788, 2021.

[24] P. Asha, L. Natrayan, B. T. Geetha et al., "IoT enabled environmental toxicology for air pollution monitoring using AI techniques," *Environmental Research*, vol. 205, p. 112574, 2022.

[25] P. Pal Pandian and I. S. Rout, "Parametric investigation of machining parameters in determining the machinability of Inconel 718 using taguchi technique and grey relational analysis," *Procedia Computer Science*, vol. 133, pp. 786–792, 2018.

[26] D. Rajamani, K. Ananthakumar, E. Balasubramanian, and J. Paulo Davim, "Experimental investigation and optimization of PAC parameters on Monel 400™ superalloy," *Materials and Manufacturing Processes*, vol. 33, no. 16, pp. 1864–1873, 2018.

[27] R. P. Zeilmann, F. Fontanive, and R. M. Soares, "Wear mechanisms during dry and wet turning of Inconel 718 with ceramic tools," *The International Journal of Advanced Manufacturing Technology*, vol. 92, no. 5-8, pp. 2705–2714, 2017.

[28] S. Yogeshwaran, L. Natrayan, S. Rajaraman, S. Parthasarathi, and S. Nestro, "Experimental investigation on mechanical properties of epoxy/graphene/fish scale and fermented spinach hybrid bio composite by hand lay-up technique," *Materials Today: Proceedings*, vol. 37, pp. 1578–1583, 2021.

[29] R. Thirumalai, J. S. Senthilkumaar, P. Selvarani, and S. Ramesh, "Machining characteristics of Inconel 718 under several cutting conditions based on Taguchi method," *Proceedings of the Institution of Mechanical Engineers, Part C: Journal of Mechanical Engineering Science*, vol. 227, no. 9, pp. 1889–1897, 2013.

[30] A. B. H. Bejaxhin, G. Paulraj, and S. Aravind, "Influence of TiN/AlCrN electrode coatings on surface integrity, removal rates and machining time of EDM with optimized outcomes," *Materials Today: Proceedings*, vol. 21, pp. 340–345, 2020.

[31] S. Montazeri, M. Aramesh, and S. C. Veldhuis, "An investigation of the effect of a new tool treatment technique on the machinability of Inconel 718 during the turning process," *The International Journal of Advanced Manufacturing Technology*, vol. 100, no. 1-4, pp. 37–54, 2019.

[32] L. Natrayan, V. Sivaprakash, and M. S. Santhosh, "Mechanical, microstructure and wear behavior of the material AA6061 reinforced SiC with different leaf ashes using advanced stir casting method," *International Journal of Engineering and Advanced Technology*, vol. 8, pp. 366–371, 2018.

[33] K. Salonitis and S. Vatousianos, "Experimental Investigation of the plasma arc cutting process," *Procedia CIRP*, vol. 3, pp. 287–292, 2012.

[34] S. A. Khan, S. L. Soo, D. K. Aspinwall et al., "Tool wear/life evaluation when finish turning Inconel 718 using PCBN tooling," *Procedia CIRP*, vol. 1, pp. 283–288, 2012.

[35] J. S. N. Raju, M. V. Depoures, and P. Kumaran, "Comprehensive characterization of raw and alkali (NaOH) treated natural fibers from _Symphirema involucratum_ stem," *International Journal of Biological Macromolecules*, vol. 186, pp. 886–896, 2021.

[36] T. Sugihara, S. Takemura, and T. Enomoto, "Study on high-speed machining of Inconel 718 focusing on tool surface topography of CBN cutting tool," *The International Journal of Advanced Manufacturing Technology*, vol. 87, no. 1-4, pp. 9–17, 2016.

[37] S. Vellaiyan, A. Subbiah, S. Kuppusamy, S. Subramanian, and Y. Devarajan, "Water in waste-derived oil emulsion fuel with cetane improver: formulation, characterization and its optimization for efficient and cleaner production," *Fuel Processing Technology*, vol. 228, p. 107141, 2022.

[38] W. Bai, A. Bisht, A. Roy, S. Suwas, R. Sun, and V. V. Silberschmidt, "Improvements of machinability of aerospace-grade Inconel alloys with ultrasonically assisted hybrid machining," *The International Journal of Advanced Manufacturing Technology*, vol. 101, no. 5-8, pp. 1143–1156, 2019.

[39] Y. Feng, T.-P. Hung, Y.-T. Lu et al., "Inverse analysis of Inconel 718 laser-assisted milling to achieve machined surface roughness," *International Journal of Precision Engineering and Manufacturing*, vol. 19, no. 11, pp. 1611–1618, 2018.

[40] Y. Feng, Y. Guo, Z. Ling, and X. Zhang, "Micro-holes EDM of superalloy Inconel 718 based on a magnetic suspension spindle system," *The International Journal of Advanced Manufacturing Technology*, vol. 101, no. 5-8, pp. 2015–2026, 2019.

[41] Z. Vagnorius and K. Sorby, "Effect of high-pressure cooling on life of SiAlON tools in machining of Inconel 718," *The International Journal of Advanced Manufacturing Technology*, vol. 54, no. 1, pp. 83–92, 2011.